How Does the Low-Frequency Variance Vary?

SHUTING YANG AND BRIAN REINHOLD

Department of Meteorology, Arrhenius Laboratory, University of Stockholm, Sweden

(Manuscript received 21 February 1990, in final form 2 August 1990)

ABSTRACT

An objective break criterion is utilized to investigate the manner in which the slowly varying component of the atmosphere (10–90 day frequency band) actually varies. It is found that a great deal of the behavior appears to be made up of relatively infrequent large amplitude transitions between quasi-persistent states. The most frequent time interval over which these transition events occur is between five and six days. The rapid speed of these events strongly suggests that some type of baroclinic instability mechanism is involved in the transition process.

1. Introduction

Perhaps one of the most interesting features revealed by Blackmon et al.'s (1977) observational analysis is the magnitude of the midlatitude atmospheric variability on time scales between 10–90 days. With the exception of the seasonal cycle, the features responsible for this so-called "low-frequency variance" account for the vast majority of the temperature and geopotential height fluctuations of the atmosphere in the Northern Hemisphere.

Both the large amplitude and apparent slowness (relative to the time scales of baroclinic development) of these features promise great potential for extended-range forecasting. Much of this potential implicitly relies upon the assumption that the phenomena themselves are inherently slowly varying; perhaps in response to some slowly varying external forcing (such as sea surface temperature anomalies) or as a result of some (as of yet unknown) sluggish internal dynamical process. However, the concept of a characteristic low-frequency time scale or the notion of "slowly varying" forcing may be misleading.

Dole (1982, 1986) has examined the composite development and breakdown of 500-mb persistent anomalies and finds that these features develop very rapidly (on a baroclinic time scale), persist on the average about 14 days (though highly variable), and collapse equally as rapidly. Horel (1985) extends these ideas to examine persistent 500-mb flow patterns irrespective of anomaly amplitude and finds that low-amplitude states are even more frequent and persistent than the high amplitude states, further documenting the occurrence of long stretches of unchanging flow. If the interannual variability is small compared to the interseasonal variability, the low-frequency flow must contain some periods of dramatic changes if it possesses simultaneously a large variance and long states of persistent flow.

The nature of these periods of active change is not easy to objectively quantify, especially if the periods of change are irregular or intermittent. Furthermore, it is difficult to associate a "time scale" in the classical sense using spectral analysis with any break, as breaks tend to be composed of several frequencies. Consequently, a spectral frequency analysis upon a primarily steady time series that has infrequent but abrupt and large changes tends to give information about the typical times scales between rapid transition events instead of information about the speed of the transition itself. In a similar manner, a time series reconstructed from a filter retaining only scales longer than x days does not eliminate break events that subjectively appear to occur over a time interval much shorter than x days. If the time interval of the breaks is shorter than the 10–90 day "time scale" generally associated with the low-frequency variance, it becomes difficult to interpret this 10–90 day value as a dynamic time scale of the weather regimes in the same sense that one associates a dynamic time scale to baroclinic instability. Instead, it may be more appropriate to link this 10–90 day value with the likelihood of transition between weather regimes.

In spite of the difficulty in objectively quantifying abrupt changes in the planetary-scale circulation, several semisubjective approaches (Sanders and Gyakum 1980; Colucci 1985; and Reinhold 1987) have fairly convincingly documented examples of abrupt shifts in weather regimes. The most thorough effort is provided by Colucci (1985), where it is noted that particular shifts in the planetary-scale regime occur following specific types of precedent explosive cyclogenesis events.

Corresponding author address: Dr. Brian Reinhold, Department of Meteorology, University of Stockholm, Arrhenius Laboratory, S-106 91 Stockholm, Sweden.

The present objective is to provide a more quantitative measure of the changes or transitions in the planetary-scale flow. In particular, one would like to be able to determine whether the flow tends to change abruptly between otherwise quasi-persistent states or whether it tends to vary in a truly slow and continuous manner.

2. Oerlemans' break criteria

To approach this question a technique developed by Oerlemans (1978) was used to objectively quantify "breaks" in a data series. This technique consists of "best-fitting" a curve that represents an idealized break to the data. Since the formulation is central for these purposes, the development given in Oerlemans (1978) is summerized here, though for further clarification the reader is referred to the original work.

Using the same notation as Oerlemans (1978), (except that S replaces β for the speed quantity) the idealized break curve is denoted by M. It has an arbitrary amplitude, speed (how steep the break actually is), and length and is expressed analytically as follows:

$$M = \sum A f_i \quad \text{where} \quad f_i = \tan^{-1}(iS)/\tan^{-1}(nS)$$

where A is the amplitude, $2n + 1$ is the total number of data points, i is an index running from $-n$ to n, and S is the speed parameter. The $\tan^{-1}(nS)$ normalizes the function such that it is plus or minus A at each end. A graph of the curve is shown in Fig. 1 for two values of S. Very fast speeds (heavy curve, $S = 1.0$) have a profile that is nearly steady over the first half of the series at amplitude $-A$, changes abruptly to amplitude A, and continues steadily at that value to the end of the series. Slow speeds (dashed curve, $S = 0.01$), on the other hand, represent nearly linear changes from $-A$ to $+A$ over the whole length of the series.

How well this transition function M fits a data series of $2n + 1$ points is given by the variance of the data series about M [denoted by $h(A)$], which is expressed by

$$h(A) = \sum (E_i - A f_i)^2/(2n + 1)$$

where E_i is the data series with the average over the interval removed. One then selects that value of A that minimizes the variance $h(A)$, which is denoted as A^*. Then A^* defines the amplitude of the break. By definition, the A that minimizes $h(A)$ is given by satisfying the condition that

$$d/dA[h(A)] = 0 \quad \text{or} \quad \sum (E_i - A^* f_i) f_i = 0.$$

Knowing A^* one can compute the minimum variance $h(A^*)$ by direct substitution.

One can then define the quality of the break by the ratio of the amplitude A^* of the break to the root mean square of the variance,

$$q = |A^*|[h(A^*)]^{-1/2}.$$

A quality of 1.0 then means that the amplitude of the break is of the same size as the fluctuations (noise) about the idealized break function M. Clearly the larger the quality, the more impressive the break will appear when actually observing the data series. Exactly how large the quality must be before it satisfies ones intuitive notions of a break is, however, ultimately subjective.

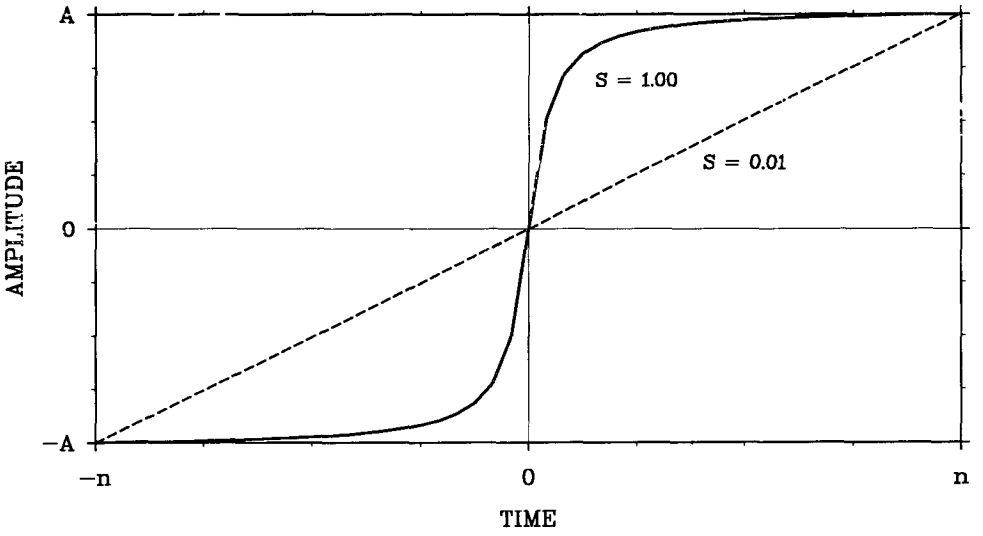

FIG. 1. Idealized break profile: Oerleman's idealized break function M for two speeds S. The dashed line is for a slow speed ($S = 0.01$), while the solid line is for a fast speed ($S = 1.0$). Though shown as a continuous function, in practice it is applied at discrete data points ranging from $-n$ to $+n$ (x axis) giving a total of $2n + 1$ points. The amplitude change goes from $-A$ to $+A$ (y axis) giving a total of $2A$ (or vice versa).

3. Dataset and method

Observations come from the National Meteorological Center (NMC) compact disk dataset put together by Mass et al. (1987). It consists of multilevel wind, temperature, and height twice daily on the NMC octagonal grid from as early as 1946 (for the surface pressure and 500-mb height) to the end of 1984. Time series of the 500-mb heights over the 39 years are generated at selected points. Missing data points are flagged. If there is only one observation missing in the sequence (during the first several years data is only once daily) it is linearly interpolated from its two neighbors and the flag is removed. Otherwise, the strings of missing data are removed from the statistics. The seasonal cycle (daily climatology) at each point is interpolated from monthly means that are computed from the 39-yr dataset on the disk. The original time series is detrended by subtracting this climatology. The data is then filtered using the Lanczos method (Duchon 1979) to retain fluctuations on the scale longer than ten days (Blackmon et al.'s 1977, low-pass filter). As discussed previously, this filtering does not remove (though it does smooth) intervals of sudden height rises or falls that occur over stretches much shorter than ten days.

The actual break analysis requires the specification of two input parameters; the speed S and the length $2n + 1$, while the output of the procedure gives two time series; the quality q and amplitude A. The position of a break is given by a local maximum in the quality q, and its corresponding amplitude A at the equivalent position in the amplitude time series.

For each value of n, a range of speeds covering abrupt breaks to linear trends is considered. The actual speed of the break in days is then both a function of the speed parameter S and the length of the series $2n + 1$. A speed category of x days is defined to mean that 75% of the total change from $-A$ to $+A$ (or vice versa) occurs in x days. The analysis then spans 20 speed categories for values of n of 20, 24, 30, 40, and 60 12-h periods, though this study will concentrate on the results from the $n = 24$ series. The 20 speed categories for the $n = 24$ series is then given by $0.9I$ where $I = 1, 2, 3, \cdots, 20$.

By applying this procedure at one given point over the whole time series for all 20 speed categories (giving 20 time series of quality and 20 time series of corresponding amplitude), that speed which maximizes the quality can be found. The final set of three time series that describes the break then consists of 1) the quality for the optimized speed, 2) the corresponding amplitude, and 3) the speed.

To this point the generation of the time series has been completely objective. However, these time series contain information about every wiggle in the data, most of which are uninteresting for our purposes. Thus only those breaks that have a quality greater than some value (usually 3.5) and a total amplitude change greater than x meters (usually 200) are considered. These two criteria are the only aspects of the analysis that are subjective.

4. Results

a. The infrequent nature of transitions

The first feature that is revealed from this analysis is that the frequency of transitions (or breaks) above a quality of 3.5 (irrespective of amplitude) is relatively rare. This is shown in Fig. 2a, which presents a contour map of the quality as a function of speed (that is, before optimization) for the winter season 1959/60 as near as possible to Dole's (1982) key point (a local maximum in the frequency of persistent anomalies) of 45°N and 170°W that the NMC octagonal grid allows. For comparison, the actual filtered and unfiltered time series of 500-mb height are shown along side of the contour plot. The contour interval is 1.5, and the lowest value shown is 3.0.

In spite of the fact that the period considered is 121 days long, there are only four (perhaps five) peaks in the quality field indicating break events. Two of the breaks are spectacular (have high quality and rapid speed). The associated time series of height clearly shows a rapid transition from one relatively constant height value to another, which then, after some time, returns to the original height level. The event is perhaps even more impressive when viewing the unfiltered height series. Of the remaining transitions, one is so close to the beginning of the plot that one is unable to view the entire event. The quality is, furthermore, marginal. The remaining event is clearly much more of a trend, and the maximum quality therefore appears in the 18-day or longer category. There is also evidence that a significant break event just before day 60 may have been missed. In the unfiltered data, there is a strong suggestion of an abrupt, very large height increase to rather steady behavior. However, in the filtered data, the preceding behavior is steadily decreasing, which does not fit the pattern of the idealized break profile. Thus the break, though fast and with very large amplitude, has a quality that lies below our subjectively chosen threshold. In general, however, it is seen that when the method indicates a break, it does provide a reasonable measure of what one would subjectively define as a break.

Figure 2b presents a Hovmöller diagram of the unfiltered data at latitude 45°N from day 45 to day 115 of the time period considered in Fig. 2a from longitude 140°E to 120°W, marking with a single line the location of Dole's (1982) critical point. (The values are interpolated from the NMC octagonal grid, and since the grid points do not fall exactly upon integer latitudes and longitudes, there will be differences between the height values between Figs. 2a and 2b.) The contour interval is 120 m, with solid and dashed lines repre-

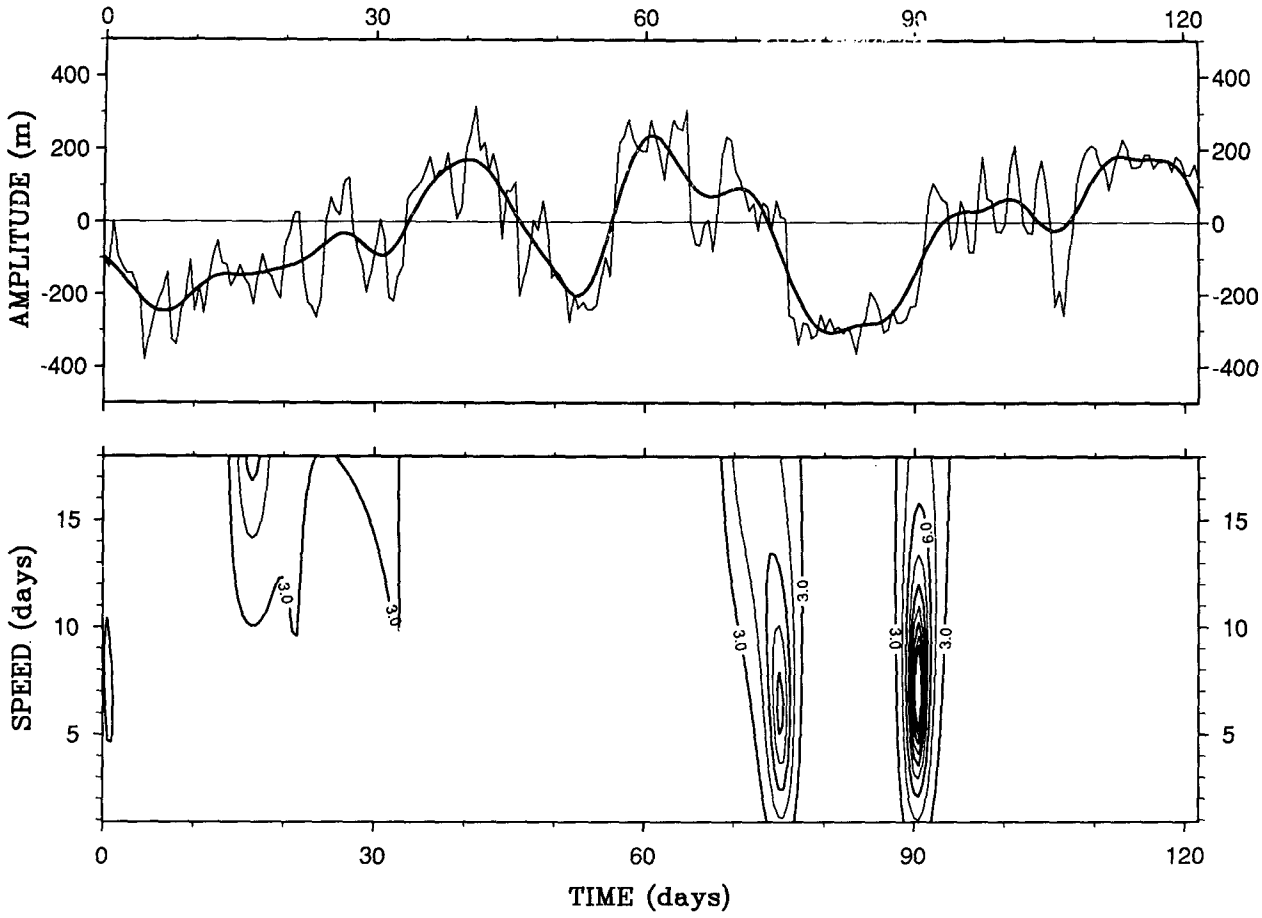

FIG. 2a. Break analysis and time series: The upper part of the figure is the filtered and unfiltered 500-mb height anomalies in meters (y axis) for the 121-day time period (x axis) from 10 November 1959 to 10 March 1960 at the point 45°N, 170°W. The lower part of the figure is a contour map of the quality of the break as a function of the break speed in days (y axis) for the corresponding 121-day time period (x axis). The contour interval is in units of 1.5, though the lowest quality shown is 3.0. The optimized break is given by that speed which maximizes the quality.

senting positive and negative anomalies, respectively. Anomalies whose magnitude exceeds 180 m are shaded, with the darker shade going to the negative values. To further ease readability, the contours begin at plus and minus 60 m instead of zero.

One can clearly see that the major height fall at about day 77 is a transition to a Pacific negative event, from what appears to be a Pacific positive event, while the breakdown of the Pacific negative event goes to a more or less "climatological" state. It can also be seen that the single point analysis does not capture the onset of the Pacific positive event near day 60 because of the continuous height falls due to the precident slow moving transient event.

b. The baroclinic time scale of transitions

Perhaps the single most important result of this analysis is the indication that transitions or breaks tend to be abrupt, or in any case, significantly quicker than indicated by the description "10–90 day low-frequency variance." This characteristic is clearly indicated in Fig. 3, which shows the number of (optimized) break events with a quality greater than 3.5 and amplitude greater than 100 m (the total change in height is therefore 200 m) in each of the 20 speed categories over the entire 39-yr dataset at the point 45°N, 170°W (heavy line) as well as for the average over ten neighboring points (thin line). In both cases, there are two distinct maxima, one being a spike at the slowest speed resolved by the 24-day length of the data segment (18 days or longer), and the other a broader peak centering at 5.4 days. On the other hand, if one sums over the neighboring categories about the aforementioned 5.4-day peak, the sum is of the same size as the 18-day and longer peak.

In order to ascertain if there is a second peak for time intervals longer than 18 days, the analysis is repeated using data strings of up to 60 days. As the data string becomes progressively longer, the spike in the

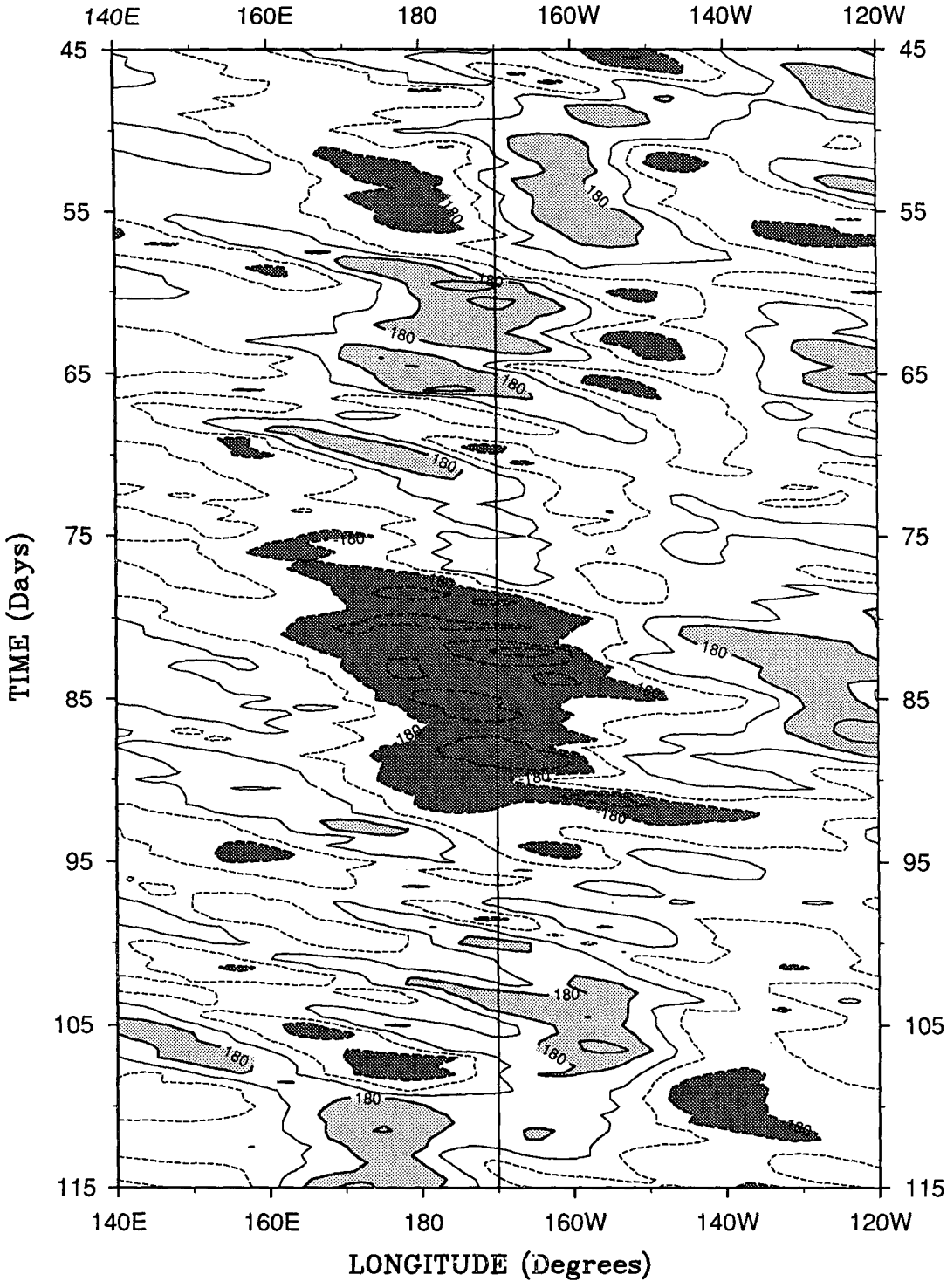

FIG. 2b. The Hovmoller diagram shows day 45 to day 115 at 45°N from 140°E to 120°W of the total 121-day time series shown in (a). Contours are every 120 m, starting at 60 m instead of 0. The solid and dashed lines are positive and negative anomalies, respectively. Anomalies exceeding 180 m of either sign are shaded, with the darker shading going to the negative anomalies.

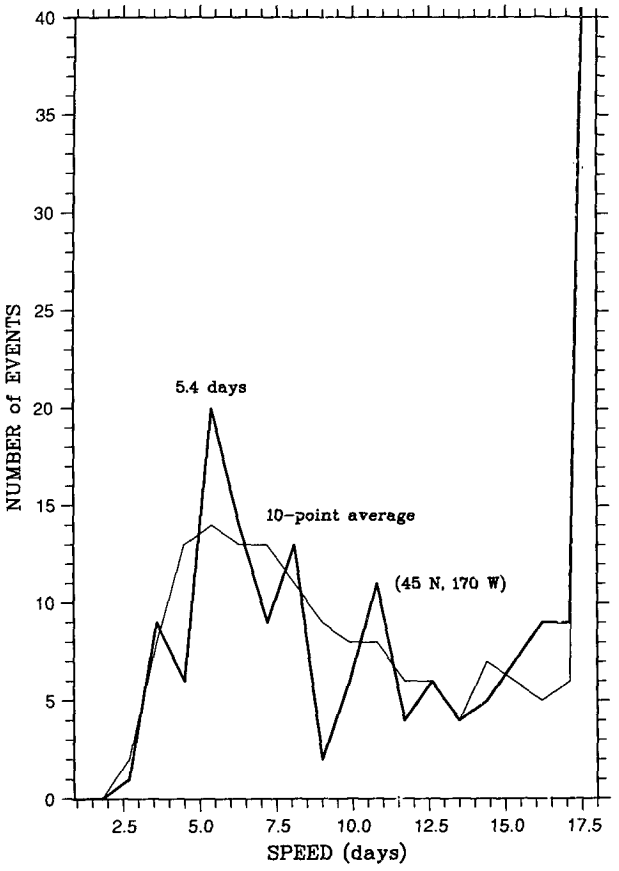

FIG. 3. Break speed distribution: The number of events is given along the y axis, while the speed of the breaks in days is given along the x axis. The heavy line is the number of break events with a quality greater than 3.5 and amplitude greater than 100 m (total change is therefore greater than 200 m) for the point 45°N, 170°W over the 39-yr data sample. The thin line gives the same break statistics described above, but is the average over 10 points surrounding the above point. The spike at the slowest time category is an artifact of the 24-day length of the data string, and thus all events that are slower than 18 days get placed into this single category.

slowest category becomes smaller and essentially disappears by about 40 days. This result implies that there is no second peak, and transition events slower than the fastest time intervals occur with about equal probability, eventually dropping off to zero as one gets out to 40 days or so. If there is a dynamical process responsible for the breaks over time intervals slower than the baroclinic time scale, we are unable to locate it by this method.

c. *Latitudinal dependence of transitions*

The analysis is then applied at several different points around the Northern Hemisphere. A special effort is made to cover the latitude circles at 40° and 50°N as best as possible given the projection. In Fig. 4 the number of break events is presented with quality greater than 3.5 and amplitude greater than 100 m as function of longitude. The heavy curve is the total number of events at all speeds. The remaining curves represent three different speed categories, fast (3.0–9.0 days denoted by a heavy line), medium (10.5–16.5 days denoted by a dashed line), and slow (18 days or more denoted by a thin line), and are individually labeled as such.

The most distinct feature of the curves is the large maxima over the eastern Pacific and eastern Atlantic oceans (corresponding to the maxima in the frequency of persistent anomalies as identified by Dole and Gordon 1983). There are more than four times as many total events in these areas than in the regions of the local minima. The distribution of rapid breaks shows an even greater asymmetry, indicating about five times as many events in the areas of maximum relative to minimum activity. In the regions of minimum break activity, the frequency of fast events decreases to the extent that medium events occur with about equal frequency. Since the peak at the slow events is an artifact of the limited length of the idealized break profile (see

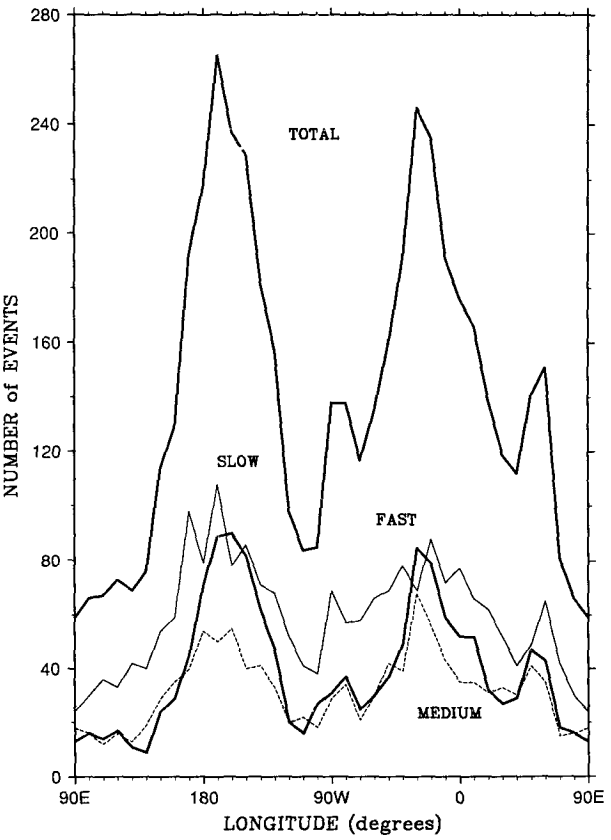

FIG. 4. Longitudinal distribution of breaks: The number of break events (y axis) is given as a function of longitude (x axis) at latitude 50°N. The four curves show the distribution for breaks of speed 3–9 days (heavy line, fast), 10.5–16.5 days (dashed line, medium), >18 days (thin line, slow), as well as all (total) events.

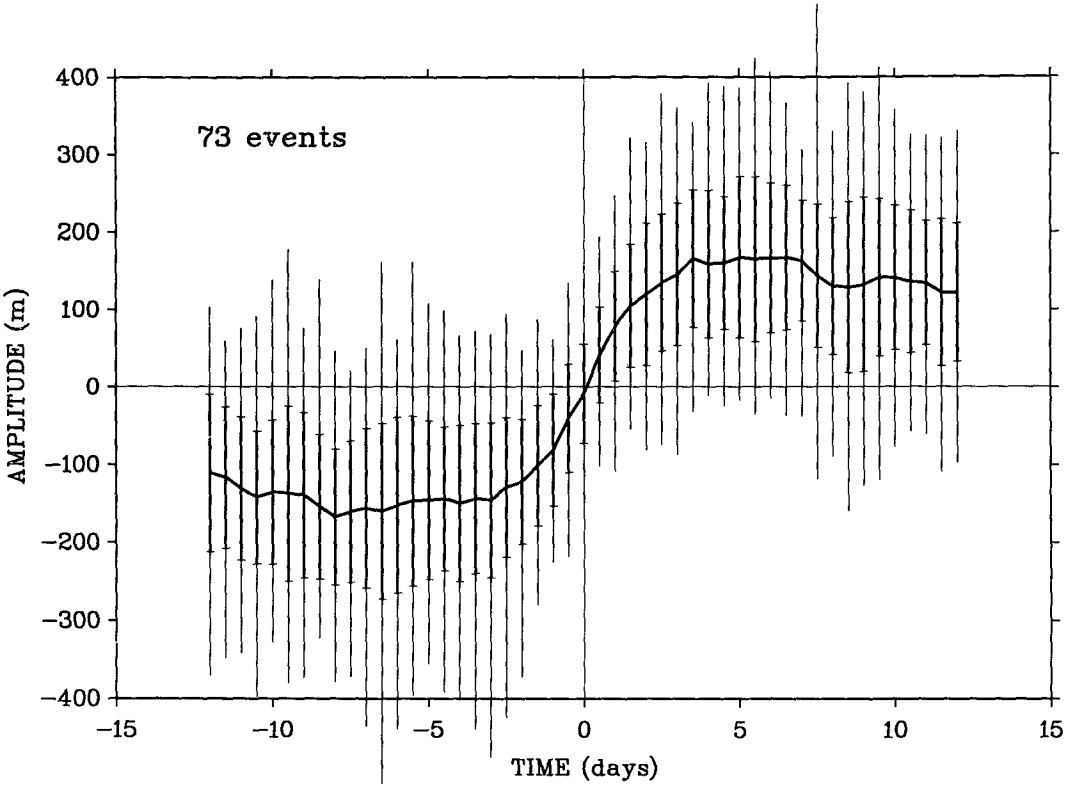

FIG. 5. Composite (fast) break profile: This figure is created by compositing the 73 events in the "fast" category at the point 45°N, 170°W. The time is in days (x axis) and the amplitude in meters (y axis). Negative events (height falls) are negated. Unfiltered data are used to create the composite, though the break point itself (denoted by day 0) is identified from the filtered data series. The heavy bars give the standard deviation of the data about the composite, while the thin bars show the extreme values of the height anomalies.

section 4b), it appears that the break speed is essentially flat or "white noise" in these areas.

On the other hand, this longitudinal dependence is not unexpected. Consistent with Dole's (1986) analysis, the regions of few breaks correspond roughly to the nodes of the large-scale pattern. "Breaks" in these areas are probably to a much greater extent due to the mobile transients.

d. Composite break

Figure 5 shows a composite break of all those events that went into the so-called "fast" category at the point 45°N, 170°W. There are a total of 73 events. Though the center of the break is identified from the quality maximum in the filtered data, the composite is obtained by concatenating the unfiltered data. Height falls are negated so that all events have the same sign. In addition the standard deviation (heavy bars) as well as the extreme values of the instantaneous heights (thin bars) are indicated about the composite. Given the data that went into the composite, the result is of no surprise. A relatively steady height for about ten days is seen, which then rises by about 300 m in six days to another quasi-steady level for the remainder of the period. Furthermore, 150 m of the rise occurs in the two days about the break point.

One feature of note is that the standard deviation and extrema are smallest during the transition period itself. Why this behavior appears is not clear. A possible explanation is that the tendencies due to the mobile baroclinic events are a part of the height rise (or fall) during the transition interval, whereas during the quasi-stationary periods, all of the height variations due to the transients contribute to the standard deviation. Thus, what appears as a variance during the steady phase of the flow is part of the process during the transition, reducing the overall variance during the changes.

There are some difficulties in being able to present a two-dimensional picture of the composite break. Though it is easy to categorize positive and negative breaks, there is no way of separating the height rise in the breakdown of Dole's (1982) Pacific negative anomaly from the height rise due to the onset of the Pacific positive anomaly. There may also be transitions directly from the Pacific negative to Pacific positive event. Clearly if all transitions are due to flipping between these two anomaly states, the composite picture

would probably be quite flat. To get a meaningful composite, one would have to get some information about the state of the flow at the time of the transition.

5. Conclusions

Oerlemans (1978) break criteria was applied to 500-mb low-frequency height data in order to get a better understanding of how the low-frequency variance actually varies. In particular, the goal was to be able to ascertain whether or not the low-frequency variance was dominated by infrequent but abrupt transitions or a mixture of gradually varying frequencies at a host of time scales. Standard spectral analysis will give similar statistics for both types of behaviors, yet the dynamical implications of the two possibilities are quite different.

The analysis indicates that breaks occur over all time intervals (or speeds) with a distinct maximum at about six days (or on the baroclinic time scale). Though slower breaks exist, no secondary longer preferred time interval could be identified. The accompanying relative rarity of breaks strongly suggests that the bulk of the low-frequency variance is indeed due to infrequent but abrupt transitions of large amplitude, but other slower processes are present as well. In addition, the peak over the time interval of six days for the transition event further suggests that the transition mechanism is associated with some type of baroclinic instability, even if the dynamics of the maintaining process are due to something else. On the other hand, the pointwise analysis method cannot distinguish between a break induced by stationary large-scale growth and a break due to a *shift* in the position of an already established large-scale disturbance. However, the feature cannot have come (in general) a great distance as the frequency of breaks, especially fast breaks, decreases rapidly as one leaves the regions of maximum low-frequency variance.

These results are consistent with the results from several other investigations. Dole's (1986) study suggests that at least the onset of the Pacific anomalies have a baroclinic precursor, and that baroclinic processes as a whole appear to be dominant in the initial stages. Karoly et al. (1989) have recently pointed out that the propagation of wave activity from the tropics into the Northern Hemisphere does not appear to play a significant role in the stationary waves. Instead, their study indicates an internal mechanism, such as instability and interactions of transients, etc. Cessi and Speranza (1985) have further indicated that the onset of Dole's (1982) persistent anomalies may be due to a large-scale baroclinic (orographic) instability.

Large-scale baroclinic (orographic) instability can be directly shown to cause weather regime transitions for an idealized case in the simple two-layer model of Reinhold and Pierrehumbert (1982). Here the parameters are chosen such that transitions between the weather regimes are very rare (yet fast). The large-scale flow is then generally stable to perturbations of the same scale until the smaller-scale transients push the large-scale wave too close to the orography, whereupon a large-scale orographic instability develops that triggers the breakdown and or onset of the weather regime. No transition is observed to occur without this instability, yet the occurrence of the instability does not guarantee a switch in regimes. (These results are published in the "Proceedings of workshop on the dynamics of long waves in the atmosphere, Kristineberg, Sweden, August 1984.) Mukougawa (1987) furthermore emphasizes the importance of large-scale baroclinic instability in weather regime transition of the aforementioned model, and concludes that this is the only energetically potent enough process to drive the transitions. In any case, the role of baroclinic instability in the variance characteristics of the low frequencies appears to be essential, even if it is unclear exactly how it manifests itself.

The inability of this analysis or standard spectral analysis to show any peak at the longer time scales supports a weather regime type of behavior for the low-frequency variance; that is, sudden transitions between multiple states of random duration. The presence of any truly low-frequency dynamical process has not, in any case, surfaced via this method, though one cannot rule out the possibility. Thus, even though there is a tremendous amount of energy at the so-called slowest frequencies, the probable mechanism of this variance in the midlatitudes does not appear to be promising for any extended range (interseasonal) forecasting method that inherently relies upon the existence of a slow dynamical process. The role of baroclinic instability appears to be a crucial element which severely complicates the problem.

Currently an attempt is being made to get a better handle upon the nature of the baroclinic processes during rapid transition events. For example, where does it start, how does it propagate, and what does it look like. In addition, it is also of interest to examine any systematic differences between those transitions that are fast and those that are "nonfast." It would also be of interest to apply this technique to the Southern Hemisphere, where the low-frequency variance is of the same order as the so-called band-pass variance (see Fig. 17 of Trenberth 1981) instead of being three times it as it is in the Northern Hemisphere (see Fig. 3 of Blackmon et al. 1977). The role of fixed zonal asymmetries is apparently much weaker in the Southern Hemisphere and thus the weather regime phenomenon is suspected to be consequently much weaker. If there is a low-frequency dynamical process (internal or external) it might be easier to locate in the Southern Hemisphere where the weather regime process may not so strongly swamp its signal. The work of Karoly et al. (1989) already suggests this possibility.

Acknowledgments. This work was supported by the Swedish Research Council (NFR) Grants G-GU 1705-307, G-GU 1705-303, and G-GU 1703-300.

REFERENCES

Blackmon, M. L., J. M. Wallace, N. C. Lau and S. L. Mullen, 1977: An observational study of the Northern Hemisphere wintertime circulation. *J. Atmos. Sci.*, **34,** 1040–1053.

Cessi, P., and Speranza, 1985: Orographic instability of nonsymmetric baroclinic flows and nonpropagating planetary waves. *J. Atmos. Sci.*, **42,** 2585–2596.

Colucci, S. J., 1985: Explosive cyclogenesis and large-scale circulation changes: implications for atmospheric blocking. *J. Atmos. Sci.*, **42,** 2701–2717.

Dole, R. M., 1982: Persistent anomalies of the extratropical Northern Hemisphere wintertime circulation. Ph.D. thesis, Massachussetts Institute of Technology.

——, 1986: The life cycles of persistent anomalies and blocking over the North Pacific. *Advances in Geophysics,* Vol. 29, Academic Press, 31–69.

——, and N. D. Gordon, 1983: Persistent anomalies of the extratropical Northern Hemisphere wintertime circulation: geographical distribution and regional persistence characteristics. *Mon. Wea. Rev.*, **111,** 1567–1586.

Duchon, C., 1979: Lancoz filtering in one and two dimensions. *J. Appl. Meteor.*, **18,** 1016–1022.

Horel, J. D., 1985: Persistence of wintertime 500-mb height anomalies over the Central Pacific. *Mon. Weather Rev.*, **113,** 2043–2048.

Karoly, D., R. Plumb and M. Ting, 1989: Examples of the horizontal propagation of quasi-stationary waves. *J. Atmos. Sci.*, **46,** 2802–2811.

Mass, C. F., H. J. Edmon, H. J. Friedman, N. R. Cheney and E. E. Recker, 1987: The use of compact disks for the storage of large meteorological and oceanographic datasets. *Bull. Amer. Meteor. Soc.*, **68,** 1556–1558.

Mukougawa, H., 1987: Instability of topographically forced Rossby waves in a two-layer model. *J. Meteor. Soc. Jpn.*, **65,** 13–25.

Oerlemans, J., 1978: An objective approach to breaks in the weather. *Mon. Wea. Rev.*, **106,** 1672–1679.

Reinhold, B. B., 1987: Weather regimes: The challenge of extended range forecasting. *Science,* **235,** 437–441.

——, and R. Pierrehumbert, 1982: Dynamics of weather regimes: quasi-stationary waves and blocking. *Mon. Wea. Rev.*, **110,** 1105–1145.

Sanders, F., and J. G. Gyakum, 1980: The synoptic-dynamic climatology of the bomb. *Mon. Wea. Rev.*, **108,** 1589–1606.

Trenberth, K., 1981: Observed Southern Hemisphere eddy statistics at 500 mb: frequency and spatial dependence. *J. Atmos. Sci.*, **38,** 2585–2605.